Published in final edited form as:
*Microcirculation*. 2012 May ; 19(4): 306–315. doi:10.1111/j.1549-8719.2012.00163.x.

# Neurovascular proximity in the diaphragm muscle of adult mice

**Diego Correa**[1,2] and **Steven S. Segal**[1,2,3,4]

[1]The John B. Pierce Laboratory, 290 Congress Avenue, New Haven, CT 06519, USA

[2]Department of Cellular and Molecular Physiology, Yale University School of Medicine, New Haven, CT 06520, USA

[3]Department of Medical Pharmacology and Physiology, University of Missouri, Columbia, MO 65212, USA

[4]Dalton Cardiovascular Research Center, Columbia, MO 65211, USA

## Abstract

**Objective—**Regional blood flow to the diaphragm muscle varies with the workload of inspiration. To provide anatomical insight into coupling between muscle fiber recruitment and oxygen supply, we tested whether arterioles are physically associated with motor nerve branches of the diaphragm.

**Methods—**Following vascular casting, intact diaphragm muscles of C57BL/6 and CD-1 mice were stained for motor innervation. Arteriolar networks and nerve networks were mapped (~2 μm resolution) to evaluate their physical proximity.

**Results—**Neurovascular proximity was similar between muscle regions and mouse strains. Of total mapped nerve lengths (C57BL/6, 70±15 mm; CD-1, 87±13 mm), 80±14% and 67±10% were ≤ 250 μm from the nearest arteriole and associated predominantly with arterioles ≤ 45 μm in diameter. Distances to the nearest arteriole encompassing 50% of total nerve length ($D_{50}$) were consistently within 200 μm. With nerve networks repositioned randomly within muscle borders, $D_{50}$ values nearly doubled ($P<0.05$). Reference lines within anatomical boundaries reduced proximity to arterioles ($P<0.05$) as they deviated from the original location of motor nerves.

**Conclusion—**Across 2 strains of mice, motor nerves and arterioles of the diaphragm muscle are more closely associated than can be explained by chance. We hypothesize that neurovascular proximity facilitates local perfusion upon muscle fiber recruitment.

### Keywords

breathing; microcirculation; muscle blood flow; phrenic nerve; proximity analysis

## Introduction

The diaphragm is the largest and most important muscle of breathing, expanding the lungs as it contracts during inspiration. Whereas the costal region of the diaphragm muscle is responsible primarily for ventilation, the crural region serves further to prevent gastroesophageal reflux (28, 30). As shown in dogs, selective activation of respective

Correspondence: Steven S. Segal, PhD, Department of Medical Pharmacology and Physiology, MA415 Medical Science Building, University of Missouri – Columbia, Columbia, MO 65212, tel: (573) 882-2553, fax: (573) 884-4276, segalss@health.missouri.edu. Current address for Dr. Correa: Skeletal Research Center, Case Western Reserve University, Cleveland OH 44106 USA diego.correa@case.edu

The authors have no disclosures to declare.

regions exerts differential effects on the rib cage and abdominal pressure (8). Dissociation between costal and crural diaphragmatic function is required during swallowing, esophageal distention and emesis. As shown in cats, such differential behavior is regulated reflexively through vagal afferents via selective inhibition of the crural muscle region (24, 29). Such distinct anatomical and functional properties have led to the diaphragm being considered as two muscles in one (8, 18, 30). The diaphragm can also be divided anatomically and functionally into complementary hemidiaphragms. In humans, distinctive motions of respective hemidiaphragms were most apparent during postural changes and during expiration in the lateral decubitus position (19). Further, with unilateral paralysis, pulmonary ventilation may be compromised through dissociating the functional integrity between hemidiaphragms (21, 34).

Across rodents, domestic and farm mammals, the diaphragm muscle is comprised of a mixture of fiber types, with mice exhibiting the highest ATPase and succinic dehydrogenase activities while having low phosphorylase activity (7). Independent studies staining for myosin ATPase isoforms in diaphragm muscles of young adult (2–4 month) C57BL/10 mice revealed a composition of ~10% Type I, ~30 % Type IIa and ~60% Type IId/x fibers (14, 15). In diaphragms of young adult C57BL/6 mice, mitochondrial volume density approaches 33% (12). These histochemical and ultrastructural profiles indicate a muscle that is able to contract forcefully with great capacity for continuous activity. Nevertheless, even with similar fiber types recruited throughout the muscle, regional heterogeneity in diaphragmatic blood flow has been attributed to corresponding differences in the workload during inspiration in rats (37), dogs (18) and ponies (27). The diaphragm can therefore be described as a single muscle comprised of distinct functional entities having both unique and complementary properties.

For limb muscles of rodents, motor nerves and feed arteries typically enter the muscle and branch away from centrally-located neurovascular pedicles (4, 35). Such physical coincidence may foster neurovascular proximity as respective structures branch to control and supply muscle fibers. For the diaphragm muscle, left and right phrenic nerves enter the thorax along ipsilateral thoracic arteries and respective structures branch to supply costal and crural regions (see Fig. 1). However the diaphragm also receives numerous vascular inputs from feed arteries located around its periphery and their arteriolar networks anastomose with each other as they branch centripetally into the muscle. In light of such a diverse topology between innervation and blood supply, it is unknown whether diaphragmatic blood flow may be influenced through a physical association between its motor innervation and its vascular supply. In so doing, the response of diaphragmatic arterioles to signals associated with muscle fiber activation [e.g., neurotransmitter release (31, 39, 40) or changes in $PO_2$ (13)] would facilitate rapid adjustments in oxygen delivery to support the aerobic production of ATP (13, 39).

Using the mouse as a model system, we tested the hypothesis that motor nerves and arteriolar networks of the diaphragm muscle physically approximate each other more closely than can be explained by chance. Our findings suggest that neurovascular proximity within the diaphragm may facilitate vasoactive signals arising from motor unit recruitment to be ‘sensed’ by nearby arterioles.

## Materials and Methods

All procedures were approved by the Animal Care and Use Committees of the John B. Pierce Laboratory and the University of Missouri and were performed in accordance with the *Guide for the Care and Use of Laboratory Animals* of the National Research Council (8th Ed., 2011)

### Vascular casting and nerve staining

To determine whether relationships under investigation were representative of the species, 2 strains of mice (C57BL/6 and CD-1; 4 males each) were studied when 3 months old. Each mouse was anesthetized with pentobarbital sodium (60 mg/kg, intraperitoneal injection) and the chest was opened using a midline incision above the xiphoid process. Upon pneumothorax, the diaphragm muscle assumed a 'flattened' position maintained by radial tension exerted by the chest wall. A 20-gauge needle was inserted through the left ventricle into the ascending aorta and secured for perfusion-fixation of the vasculature followed immediately by perfusion with a silicone-based casting compound (Microfil; Flowtech, Carver, MA) that was allowed to set overnight at 4 °C (4). While viewing through a stereomicroscope, the entire diaphragm muscle was excised while preserving the costal and crural insertions and then pinned to approximate *in situ* dimensions during pneumothorax. Motor axons were stained with Sudan Black B and preparations were cleared in glycerin for 3 days while maintained at 4 °C (35).

### Motor end plate staining

To determine the pattern of motor endplate distribution, diaphragm muscles from 4 additional male mice (2 each for C57BL/6 and CD-1) were pinned at in situ dimensions and motor end plates were stained for cholinesterase activity after staining motor nerves with Sudan B black. Following staining, muscles were immersed in 50% glycerin for 4 days at 4 °C to clear the tissue and facilitate visualization of motor axons and NMJs on individual muscle fibers (35).

### Network mapping

Vascular and neural networks were imaged on a Nikon microscope (E600; Tokyo, Japan) using 10X and 20X objectives (numerical aperture, 0.30 and 0.50 respectively) coupled to a cooled charge-coupled device megapixel camera (Optronics Microfire; Goleta, CA). The imaging system was interfaced to a motorized stage (Ludl; Hawthorne, NY) for 3-dimensional mapping using a Neurolucida system (Microbrightfield; Williston, VT). Images were displayed on a digital monitor at final magnification 380X and 760X respectively. Briefly, arteriolar networks were mapped beginning with the entry of each feed artery into the muscle and included all arteriolar branches through the terminal arterioles; completeness of vascular casts was confirmed visually by the absence of blunt ends. Complete motor nerve networks were mapped beginning with association of the phrenic nerve onto the thoracic surface of the diaphragm and nerve branches were followed up to single axon divisions near motor endplates. Vascular and nerve networks were mapped on the same day to ensure that spatial relationships between respective networks were maintained throughout data acquisition for each preparation. Respective networks were thereby digitized into X-Y-Z coordinates with a spatial resolution of ≤2 μm (4).

### Proximity analysis

Proximity analysis between motor nerve and arteriolar networks was performed using Neurolucida software (4). Briefly, at each micron along the nerve network, the software calculates the distance to the nearest arteriole and its diameter at that site. User-designated intervals define the relationship for separation distance and vessel diameter relative to the total length of the mapped nerve network. In accord with proximity analyses of locomotor muscles from C57BL/6 mice (4), the intervals for arteriolar diameters were 15 μm while those for separation distance was 50 μm.

### Anatomical boundary controls

To test whether the proximity analysis between neural and vascular networks represented actual association with each other or were simply a consequence of both networks constrained to the same anatomical boundaries, two sets of control analyses were performed.

**Repositioned nerve networks—**Proximity analyses were repeated for each muscle after the entire nerve network was repositioned in its original tissue plane within muscle boundaries while maintaining the vascular network in its original location. Analogous to the $EC_{50}$ in a concentration-response curve, cumulative frequency plots (ogives) were constructed to determine values for "$D_{50}$" to represent the distance to nearest arteriole within which 50% of the total nerve length occurred (4). For statistical analyses, $D_{50}$ values determined for actual network maps were compared to those for repositioned network maps.

**Independent reference lines—**A set of nine parallel reference lines, each representing ~75% of total nerve length associated with the costal region of the left hemidiaphragm, were oriented with respect to the "tissue planes" in which nerves and vessels were actually located (illustrated in Figures 6A and 6B). The positioning of these reference lines corresponded to: (a) adjacent to the thoracic surface of the muscle (i.e., closest to the plane in which the phrenic nerve network coursed); (b) midway through the muscle thickness (corresponding to the plane in which arteriolar networks coursed); and (c) adjacent to the abdominal muscle surface, corresponding to the deepest plane of the muscle. Within each tissue plane, reference lines were positioned along or below the corresponding segment of the phrenic nerve, or were shifted laterally by 45% and by 90% of the distance to the costal boundary of the muscle. Proximity analysis was performed for each reference line relative to the vascular network within that region of the muscle and respective $D_{50}$ values were compared with reference to the $D_{50}$ value determined for actual nerve networks.

### Statistical analyses

Data were analyzed using SigmaStat software (Systat Inc., San Jose, CA). Student's paired and unpaired t-tests were used to compare total nerve lengths between C57BL/6 and CD-1 mice and for comparing $D_{50}$ values before and after repositioning nerve networks. Analysis of Variance with Holm-Sidak post hoc tests were used to compare $D_{50}$ values for independent reference lines. Summary data are presented as means ± S.D. Differences were accepted as statistically significant with $P < 0.05$.

## Results

### Topology of motor innervation and vascular supply

A representative illustration of a mouse diaphragm preparation viewed from the thoracic surface is shown in Figure 1; motor endplate bands revealed with cholinesterase staining are superimposed on arteriolar and neural networks. In light of regional differences in the anatomical and functional properties of the diaphragm, respective networks were analyzed with respect to the entire diaphragm muscle, for left and right hemidiaphragms, and for costal versus crural regions.

**General features—**The left and right phrenic nerves contact the diaphragm near the mid-region of the muscle (Fig. 1, blue arrows) then divide into respective costal (anterior and posterior) and crural branches, which course along the thoracic surface. Motor nerve branches typically course along the midline of each muscle region, perpendicular to the muscle fibers. The width of the motor endplate band reflects terminal axons extending laterally in each direction as they branch from the nerve bundle to form neuromuscular junctions. Thus nerve networks approximate the 'midline' of the distribution of

neuromuscular junctions. Distinguishing features of the vascular supply include multiple feed arteries entering around the muscle periphery with numerous anastomoses between respective arteriolar networks as they branch centripetally. Respective feed arteries arise from the musculophrenic and pericardiophrenic branches of the superior phrenic artery (supplying the costal region) and branches of the inferior phrenic arteries (supplying the posterior crural region). Once feed arteries enter the muscle, they give rise to arteriolar networks whose primary branches lie approximately mid-way through the muscle thickness (~200 μm); i.e. arteriolar networks are located in a plane ~100 μm below that of phrenic nerves if preparations are viewed on edge (not shown).

**Proximity analysis—**Three-dimensional plots illustrate relationships among the separation distance between nerve fibers and their nearest arteriole with respect to vessel diameter. As shown for C57BL/6 mice (Fig. 2) and for CD-1 mice (Fig. 3), the majority of nerve length is associated with arterioles < 45 μm in diameter and located within ~200 μm. These associations are apparent in all muscle regions (Figs. 2 and 3, panels B–E). Overall, a similar pattern of neurovascular proximity was found between mouse strains as well as between respective muscle regions within each strain. In the crural region of all preparations, a smaller peak of nerve length associated with vessel diameters of 60–75 μm corresponded to the inferior phrenic arteries as they enter the muscle and cross to the costal region near the crural branch of the phrenic nerve (Fig. 1).

Total lengths of phrenic nerve branches mapped for entire diaphragm muscles were 70 ± 15 mm (C57BL/6) and 87 ± 13 mm (CD-1). The majority of phrenic innervation was associated with intermediate and distal arterioles 15–30 μm in diameter for both C57BL/6 mice (Fig. 4A) and CD-1 mice (Fig. 4B), with 84 ± 2% (C57BL/6) and 80±10% (CD-1) of total nerve length associated with vessels ≤ 45 μm diameter (Figs. 4C and 4D, respectively). In C57BL/6 mice, 80±14% of total nerve length was within 250 μm of the nearest arteriole while in CD-1 mice 67±10% was within this distance (Fig. 4B); respective values were not significantly different ($P > 0.05$) between strains.

### Anatomical boundary controls

**Repositioned nerve networks—**The $D_{50}$ value (i.e., the distance to the nearest arteriole within which 50% of total nerve length resides) was 155±30 μm for C57BL/6 and 199±22 μm for CD-1 mice (Fig. 5). After repositioning the neural network within muscle boundaries (with arteriolar networks maintained in their original position as mapped), respective $D_{50}$ values nearly doubled (286 ± 77 μm and 386 ± 64 μm, respectively; both $P<0.05$ vs. original, Fig. 5). There were no significant differences between mouse strains either before or after repositioning networks (Fig. 5).

**Independent reference lines—**The positioning of reference lines is illustrated in Figure 6. Line 1 resulted in $D_{50}$ values (144 ± 31 μm) similar to values determined for the actual nerves (155 ± 30 μm), consistent with Line 1 approximating the position of the actual nerve segments being referenced. Line 2 (located below line 1 midway through muscle thickness) approximated the location of arterioles and had a significantly ($P<0.05$) closer $D_{50}$ value (85 μm) than control. With the exception of reference Line 5 (lateral to Line 2 and diagonal to Line 1), all other reference lines resulted in $D_{50}$ values significantly greater ($P<0.05$) than the actual innervation (Fig. 6C).

## Discussion

The present study illustrates a physical association between motor innervation and arterioles of the diaphragm muscle in 2 strains of mice. Neurovascular proximity apparent for the entire muscle (Fig. 1) is maintained within each region of the diaphragm whether considered

as costal versus crural or as respective hemidiaphragms (Figs. 2 and 3) and its consistency between mouse strains implies that it is a general feature of the healthy murine diaphragm. Neurovascular association was greatest for arterioles 15–30 μm in diameter that coursed within 250 μm of the nearest motor nerve (Fig. 4). Importantly, neurovascular proximity decreased significantly when nerve networks were repositioned within anatomical boundaries (Fig. 5) or when an independent reference line was shifted within a muscle region (Fig. 6). These findings indicate that the physical proximity between arterioles that supply muscle fibers of the diaphragm and motor nerves that govern their contractile activity is not the result of a random association between two independent networks within the muscle. Instead, we hypothesize that neurovascular proximity may contribute to the local control of blood flow during motor unit recruitment in the diaphragm muscle.

## Neurovascular proximity

Physical association between nerves and blood vessels is promoted during development by shared guidance molecules and complementary synthesis of growth factors. For example, whereas vascular endothelial growth factor (VEGF) was discovered in light of its ability to enhance permeability (36), it also promotes angiogenesis along with growth and survival of neurons. In turn, nerve growth factor promotes endothelial cell growth and proliferation (5, 22). The physical associations between respective systems that are recognized in adult mammals include the vascular supply to nerves [vasa nervorum (1)] and autonomic innervation of the vasculature [nervi vasorum (23)], a relationship also guided by molecular cues (26). In hamsters, ectopic reattachment of the spinal accessory nerve to the cheek pouch retractor muscle resulted in axon sprouting and angiogenesis originating from the implanted nerve stump and its vasa nervorum, with VEGF released from regenerating microvessels promoting neurotization (3). Following spinal cord injury in the mouse, a physical association between nerves and vessels was also apparent during the first 2 weeks post-injury, where axon sprouts proliferated in proximity to newly-formed blood vessels which appeared to exert a trophic effect on regenerating axons during this initial period of recovery (9). Thus, respective systems in the adult respond to injury in a manner complementary to that seen during development, thereby promoting mutual restoration of function.

In studying spatial relationships among neuromuscular junctions and microvessels in the cremaster muscle of hamsters, the mean distance between NMJs and arterioles was typically ~100 μm (31). While these earlier findings are consistent with the present observations, our proximity analysis of mapping utilizes the entire motor nerve network as a continuous and comprehensive reference (e.g., for determining $D_{50}$ values in Figs. 4 and 5) in contrast sampling discrete entities based upon stereological grids positioned over the tissue (31). Further, maintaining the integrity of complete nerve and arteriolar networks enabled us to perform boundary controls to ascertain whether their physical association could be explained simply by chance.

## Boundary controls

Nerves and vessels may be “forced” into physical proximity through being constrained to the same anatomical boundaries. To determine whether the physical association apparent for motor innervation and arteriolar supply observed throughout the diaphragm muscle simply reflected a random association between the two networks within a defined space, two approaches were employed. First, the nerve network was repositioned relative to the vascular network within the anatomical boundaries of the muscle and within its native tissue plane. Using $D_{50}$ values for reference, separation distance nearly doubled after repositioning (Fig. 5), reflecting a significant reduction in the association between respective networks. Our second approach positioned an independent reference line within the left costal region

of the diaphragm to explore the potential for a spatial gradient of association between motor nerves and arterioles. For each muscle, the reference line approximated the length of the nerve segment determined within that region of the diaphragm and was repositioned in 9 locations to encompass three anatomically defined planes at 3 defined distances across the width of the muscle (Fig. 6). Our finding that Line 1 (which replicates the original location of innervation) had $D_{50}$ values similar those determined for actual nerves supports this approach. Additional validation comes from Line 2, which was positioned below Line 1 in the same plane as the arteriolar network and exhibited $D_{50}$ values significantly less than Line 1, as would be predicted by being artificially closer to arterioles than determined for nerves in the actual muscle. With the exception of Line 5, the remaining reference lines showed a progressive and significant increase in $D_{50}$ relative to Line 1 (Fig. 6), consistent with a spatial gradient of neurovascular proximity. In turn, the similarity in $D_{50}$ for Line 5 compared to Line 1 is attributable to Line 5 being in the same plane as arterioles, albeit lateral to Line 2. Complementary findings in both strains of mice (Fig. 5) imply that the inherent proximity of respective networks is significantly closer than would be achieved by random positioning within the anatomical boundaries of the diaphragm muscle.

## Key features of neurovascular proximity in the mouse diaphragm

Using methods similar to those employed here, neurovascular proximity was apparent in murine locomotor skeletal muscles having diverse morphology and neurovascular topology (4). Limb muscles (e.g., the gracilis and gluteus maximus) tend to have divergent branching arteriolar networks originating from feed arteries associated with their neurovascular pedicles. An exception is the spinotrapezius muscle, which in addition to its neurovascular pedicle, has multiple feed arteries around its periphery and extensive anastomoses between arteriolar networks (4). As shown in Figure 1, a similar arrangement is apparent for the diaphragm muscle, albeit on a larger scale. However, in contrast to locomotor muscles studied thus far, the left and right phrenic nerves approach respective hemidiaphragms surface well removed from the multitude of peripheral vascular inputs (Fig. 1). Thus the physical association between diaphragmatic arterioles and motor nerves cannot be attributed to the continuation of a pre-established relationship of respective structures prior to entering the muscle.

Our regional analyses were performed to determine whether the association of motor nerves and blood vessels varied according the multifunctional properties of the muscle (8, 18, 30). Comparison of respective hemidiaphragms was based upon each having autonomous motor innervation and thus capable of independent function (19, 34). A complementary analysis divided the muscle in costal and crural regions based upon distinct functional roles during ventilation (8, 18) and the unique role of the crural diaphragm in preventing gastroesophageal reflux (28, 30). Remarkably, the physical association between motor nerves and arterioles was found throughout the diaphragm irrespective of the muscle region or its functional role. Thus, even with motor unit recruitment encompassing large regions of the diaphragm muscle as shown in rats (20), the actual work done within respective muscle regions is a principal determinant of blood flow and oxygen delivery (18, 27, 37). Additional studies are required to determine whether neurovascular proximity illustrated here in the mouse is manifest in larger species (8, 24, 27).

A notable feature of this study is the association of motor nerves predominantly with arterioles having diameters of 15–30 μm (Figs. 4A and 4B). In contrast, for mouse limb muscles the association of motor nerves with arterioles occurred over a broader range of vessel diameters (15–60 μm) (4). Nevertheless, our observations in the diaphragm muscle are consistent with limb muscles in that the majority of nerve length was located within ~200 μm of the nearest arteriole [Fig. 5 and (4)].

## Functional implications of neurovascular interaction

As with muscles of locomotion, the ability of the diaphragm to sustain contractile performance depends critically upon blood flow to its active muscle fibers (16) and this dependence increases with the demands of exercise (33). In addition to energy production and metabolite removal, diaphragmatic blood flow is affected dramatically by changes in length, tension and pressures it exerts during the respiratory cycle (2, 17, 32). The multiple vascular sources entering the diaphragm collectively provide collateral sources of perfusion to respective costal and crural muscle regions (6, 25). Indeed, the numerous arteriolar anastomoses within the muscle (Fig. 1) are consistent with a dynamic vascular network that can deliver blood to regions having the greatest energetic demand and mechanical advantage (18, 27, 33, 37). As the present findings are based upon topological analyses of motor innervation and arteriolar supply, the functional consequences of neurovascular proximity remain to be defined. Nevertheless, the present anatomical data lead us to hypothesize that nearby arterioles may sense the recruitment of muscle fiber activation [e.g., via neurotransmitter release (31, 39, 40) or changes in $PO_2$ (13)] as a stimulus contributing to rapid adjustments of the resistance network in the local control of blood flow and oxygen delivery.

The present study provides a novel reference for investigating how neurovascular proximity may be altered in diseased states. Regional differences in blood flow to the diaphragm are maintained during emphysema, where higher blood flows are associated with greater energetic demands of ventilation at increased lung volumes (38). Similar responses are predicted for hyperinflation accompanying diseases of the airways (21). Diaphragmatic function is compromised in such neuromuscular disorders as muscular dystrophy and myasthenia gravis, as well as by structural abnormalities of the chest wall or lungs (21). Each condition would be expected to have differential effects on diaphragmatic contractile function and regional blood flow. Moreover, in light of diabetic neuropathy of the phrenic nerve (10, 11) and the pleiotropic actions of VEGF on neurogenesis and angiogenesis being implicated in an array of neurological disorders (5), greater understanding neurovascular topology may provide needed insight into the pathophysiology of these diseases as well as in developing more effective therapeutic strategies.

## Summary and conclusion

The recruitment of muscle fibers and the supply of oxygen are well coupled through a wide range of contractile performance and energetic requirements. However the spatial relationships between the control elements of respective systems have not been well defined. The present findings are the first to investigate the proximity of motor innervation to arteriolar supply in the mammalian diaphragm using the adult mouse as a model system. Across 2 strains of mice, our findings illustrate that neurovascular proximity is manifest throughout each region of the diaphragm muscle and this physical association cannot be explained by random approximation of respective networks within anatomical boundaries. Feed arteries enter at multiple sites around the periphery of the diaphragm and give rise to anastomotic arteriolar networks within the muscle, indicating that each region of the diaphragm can receive blood flow from multiple sources according to local demand. In contrast to this peripheral origin of arteriolar networks, motor innervation originates centrally from the phrenic nerves. Nevertheless, neurovascular proximity is established as motor nerve branches project to neuromuscular junctions within each muscle region. Based upon the anatomical relationships defined here, we hypothesize that the physical association between motor innervation and arteriolar supply can promote local perfusion of the diaphragm muscle according to the recruitment of its muscle fibers.

## Acknowledgments

Grants: This research was supported by NIH grants R01-HL056786 and R01-HL086483. DC was supported by 2T32-GM07527

The authors acknowledge the outstanding technical assistance of Chady H. Hakim and are grateful to Prof. D.W. Slaaf for recommending the independent reference line analysis used in Figure 6.

## Abbreviations

| | |
|---|---|
| **ATP** | adenosine triphosphate |
| **$D_{50}$** | distance to nearest arteriole within which 50% of total nerve length occurs, vascular endothelial growth factor (VEGF) |

## References

1. Amenta F, Mione MC, Napoleone P. The autonomic innervation of the vasa nervorum. J Neural Transm. 1983; 58:291–297. [PubMed: 6663303]
2. Bark H, Scharf SM. Diaphragmatic blood flow in the dog. J Appl Physiol. 1986; 60:554–561. [PubMed: 3949660]
3. Bearden SE, Segal SS. Microvessels promote motor nerve survival and regeneration through local VEGF release following ectopic reattachment. Microcirculation. 2004; 11:633–644. [PubMed: 15726831]
4. Bearden SE, Segal SS. Neurovascular alignment in adult mouse skeletal muscles. Microcirculation. 2005; 12:161–167. [PubMed: 15824038]
5. Carmeliet P, Storkebaum E. Vascular and neuronal effects of VEGF in the nervous system: implications for neurological disorders. Semin Cell Dev Biol. 2002; 13:39–53. [PubMed: 11969370]
6. Comtois A, Gorczyca W, Grassino A. Anatomy of diaphragmatic circulation. J Appl Physiol. 1987; 62:238–244. [PubMed: 3558184]
7. Davies AS, Gunn HM. Histochemical fibre types in the mammalian diaphragm. J Anat. 1972; 112:41–60. [PubMed: 4263892]
8. De Troyer A, Sampson M, Sigrist S, Macklem PT. Action of costal and crural parts of the diaphragm on the rib cage in dog. J Appl Physiol. 1982; 53:30–39. [PubMed: 7118646]
9. Dray C, Rougon G, Debarbieux F. Quantitative analysis by in vivo imaging of the dynamics of vascular and axonal networks in injured mouse spinal cord. Proc Natl Acad Sci U S A. 2009; 106:9459–9464. [PubMed: 19470644]
10. Fazan VP, Rodrigues Filho OA, Jordao CE, Moore KC. Phrenic nerve diabetic neuropathy in rats: unmyelinated fibers morphometry. J Peripher Nerv Syst. 2009; 14:137–145. [PubMed: 19691536]
11. Fisher MA, Leehey DJ, Gandhi V, Ing T. Phrenic nerve palsies and persistent respiratory acidosis in a patient with diabetes mellitus. Muscle Nerve. 1997; 20:900–902. [PubMed: 9179167]
12. Gamboa JL, Andrade FH. Mitochondrial content and distribution changes specific to mouse diaphragm after chronic normobaric hypoxia. Am J Physiol Regul Integ Physiol. 2010; 298:R575–583.
13. Geer CM, Behnke BJ, McDonough P, Poole DC. Dynamics of microvascular oxygen pressure in the rat diaphragm. J Appl Physiol. 2002; 93:227–232. [PubMed: 12070209]
14. Gregorevic P, Plant DR, Leeding KS, Bach LA, Lynch GS. Improved contractile function of the mdx dystrophic mouse diaphragm muscle after insulin-like growth factor-I administration. Am J Pathol. 2002; 161:2263–2272. [PubMed: 12466140]
15. Guido AN, Campos GE, Neto HS, Marques MJ, Minatel E. Fiber type composition of the sternomastoid and diaphragm muscles of dystrophin-deficient mdx mice. Anat Rec. 2010; 293:1722–1728.
16. Hussain SN. Regulation of ventilatory muscle blood flow. J Appl Physiol. 1996; 81:1455–1468. [PubMed: 8904553]

17. Hussain SN, Magder S. Diaphragmatic intramuscular pressure in relation to tension, shortening, and blood flow. J Appl Physiol. 1991; 71:159–167. [PubMed: 1917737]

18. Johnson RL Jr, Hsia CC, Takeda S, Wait JL, Glenny RW. Efficient design of the diaphragm: distribution of blood flow relative to mechanical advantage. J Appl Physiol. 2002; 93:925–930. [PubMed: 12183487]

19. Kiryu S, Loring SH, Mori Y, Rofsky NM, Hatabu H, Takahashi M. Quantitative analysis of the velocity and synchronicity of diaphragmatic motion: dynamic MRI in different postures. Magn Reson Imaging. 2006; 24:1325–1332. [PubMed: 17145404]

20. Krnjevic K, Miledi R. Motor units in the rat diaphragm. J Physiol. 1958; 140:427–439. [PubMed: 13514716]

21. Laghi F, Tobin MJ. Disorders of the respiratory muscles. Am J Respir Crit Care Med. 2003; 168:10–48. [PubMed: 12826594]

22. Lazarovici P, Marcinkiewicz C, Lelkes PI. Cross talk between the cardiovascular and nervous systems: neurotrophic effects of vascular endothelial growth factor (VEGF) and angiogenic effects of nerve growth factor (NGF)-implications in drug development. Curr Pharm Des. 2006; 12:2609–2622. [PubMed: 16842161]

23. Lincoln J, Milner P, Appenzeller O, Burnstock G, Qualls C. Innervation of normal human sural and optic nerves by noradrenaline- and peptide-containing nervi vasorum and nervorum: effect of diabetes and alcoholism. Brain Res. 1993; 632:48–56. [PubMed: 7511981]

24. Liu J, Yamamoto Y, Schirmer BD, Ross RA, Mittal RK. Evidence for a peripheral mechanism of esophagocrural diaphragm inhibitory reflex in cats. Am J Physiol Gastrointest Liver Physiol. 2000; 278:G281–288. [PubMed: 10666053]

25. Lockhat D, Magder S, Roussos C. Collateral sources of costal and crural diaphragmatic blood flow. J Appl Physiol. 1985; 59:1164–1170. [PubMed: 4055596]

26. Long JB, Jay SM, Segal SS, Madri JA. VEGF-A and Semaphorin3A: modulators of vascular sympathetic innervation. Dev Biol. 2009; 334:119–132. [PubMed: 19631637]

27. Manohar M. Costal vs. crural diaphragmatic blood flow during submaximal and near-maximal exercise in ponies. J Appl Physiol. 1988; 65:1514–1519. [PubMed: 3182515]

28. Mittal RK. The crural diaphragm, an external lower esophageal sphincter: a definitive study. Gastroenterology. 1993; 105:1565–1567. [PubMed: 8224664]

29. Oyer LM, Knuth SL, Ward DK, Bartlett D Jr. Reflex inhibition of crural diaphragmatic activity by esophageal distention in cats. Respir Physiol. 1989; 77:195–202. [PubMed: 2781162]

30. Pickering M, Jones JF. The diaphragm: two physiological muscles in one. Journal of anatomy. 2002; 201:305–312. [PubMed: 12430954]

31. Pierzga JM, Segal SS. Spatial relationships between neuromuscular junctions and microvessels in hamster cremaster muscle. Microvasc Res. 1994; 48:50–67. [PubMed: 7990723]

32. Poole DC, Mathieu-Costello O. Capillary and fiber geometry in rat diaphragm perfusion fixed in situ at different sarcomere lengths. J Appl Physiol. 1992; 73:151–159. [PubMed: 1506362]

33. Poole DC, Sexton WL, Behnke BJ, Ferguson CS, Hageman KS, Musch TI. Respiratory muscle blood flows during physiological and chemical hyperpnea in the rat. J Appl Physiol. 2000; 88:186–194. [PubMed: 10642380]

34. Qureshi A. Diaphragm paralysis. Semin Respir Crit Care Med. 2009; 30:315–320. [PubMed: 19452391]

35. Segal SS, Cunningham SA, Jacobs TL. Motor nerve topology reflects myocyte morphology in hamster retractor and epitrochlearis muscles. J Morphol. 2000; 246:103–117. [PubMed: 11074578]

36. Senger DR, Galli SJ, Dvorak AM, Perruzzi CA, Harvey VS, Dvorak HF. Tumor cells secrete a vascular permeability factor that promotes accumulation of ascites fluid. Science. 1983; 219:983–985. [PubMed: 6823562]

37. Sexton WL, Poole DC. Costal diaphragm blood flow heterogeneity at rest and during exercise. Respir Physiol. 1995; 101:171–182. [PubMed: 8570919]

38. Sexton WL, Poole DC. Effects of emphysema on diaphragm blood flow during exercise. J Appl Physiol. 1998; 84:971–979. [PubMed: 9480959]

39. VanTeeffelen JW, Segal SS. Rapid dilation of arterioles with single contraction of hamster skeletal muscle. Am J Physiol Heart Circ Physiol. 2006; 290:H119–127. [PubMed: 16100250]

40. Welsh DG, Segal SS. Coactivation of resistance vessels and muscle fibers with acetylcholine release from motor nerves. Am J Physiol. 1997 Jul; 273(1 Pt 2):H156–63. [PubMed: 9249486]

## Perspectives

The diaphragm muscle is the most important muscle for breathing yet the physical association between motor innervation controlling diaphragmatic contraction and the microcirculation controlling oxygen delivery to its muscle fibers is undefined. We investigated whether physical proximity exists between motor nerves and arterioles within diaphragm muscle. In 2 strains of mice, we find that motor nerves and arterioles are more closely associated with each other than can be explained by chance, providing a foundation for exploring how these relationships may influence blood flow control and whether they are altered with injury, disease or aging.

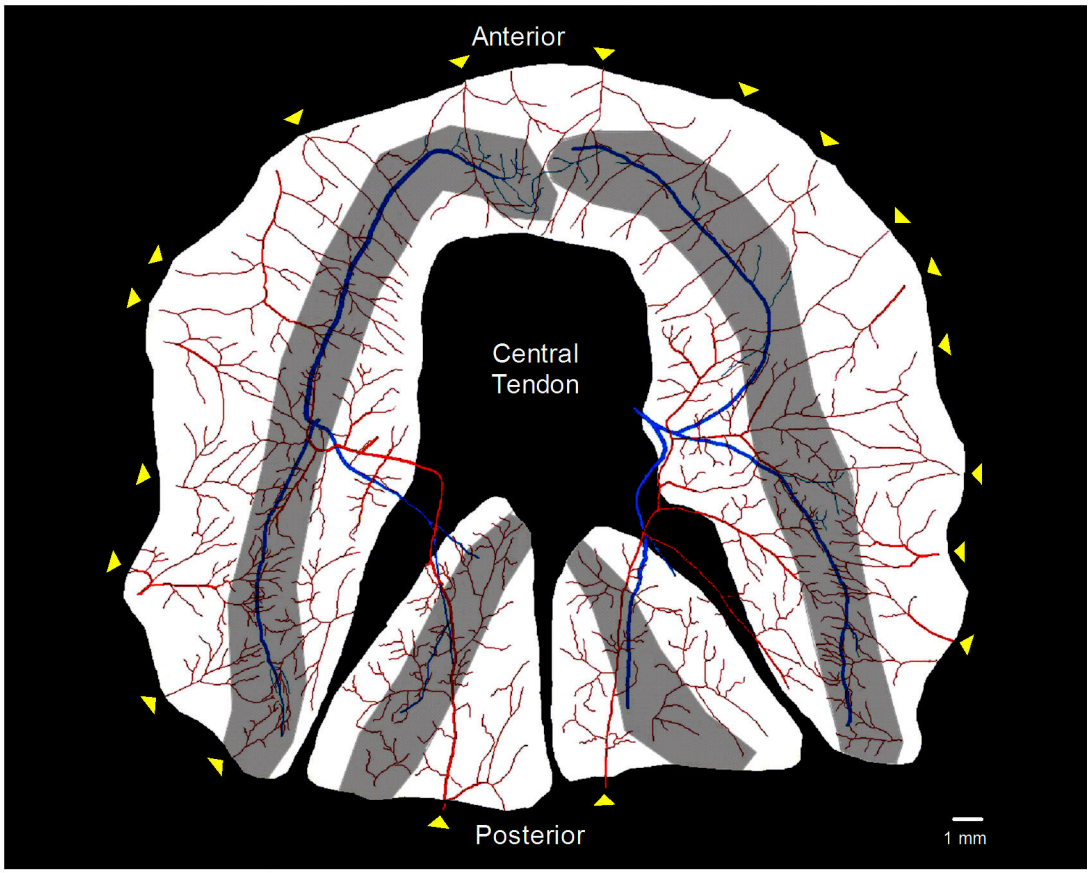


**Figure 1. Diaphragm muscle preparation**

Reconstructed image of the diaphragm muscle preparation from a C57BL/6 mouse as viewed from the thoracic cavity. The vascular supply (arteriolar networks) is shown in red, phrenic nerves in blue and motor endplate regions are shaded gray. Note numerous anastomoses among arteriolar networks supplied by multiple feed arteries entering around periphery of the diaphragm (yellow arrowheads) arising from respective branches of the phrenic arteries. In contrast, left and right phrenic nerves enter near the central region of the costal diaphragm and branch into respective muscle regions.

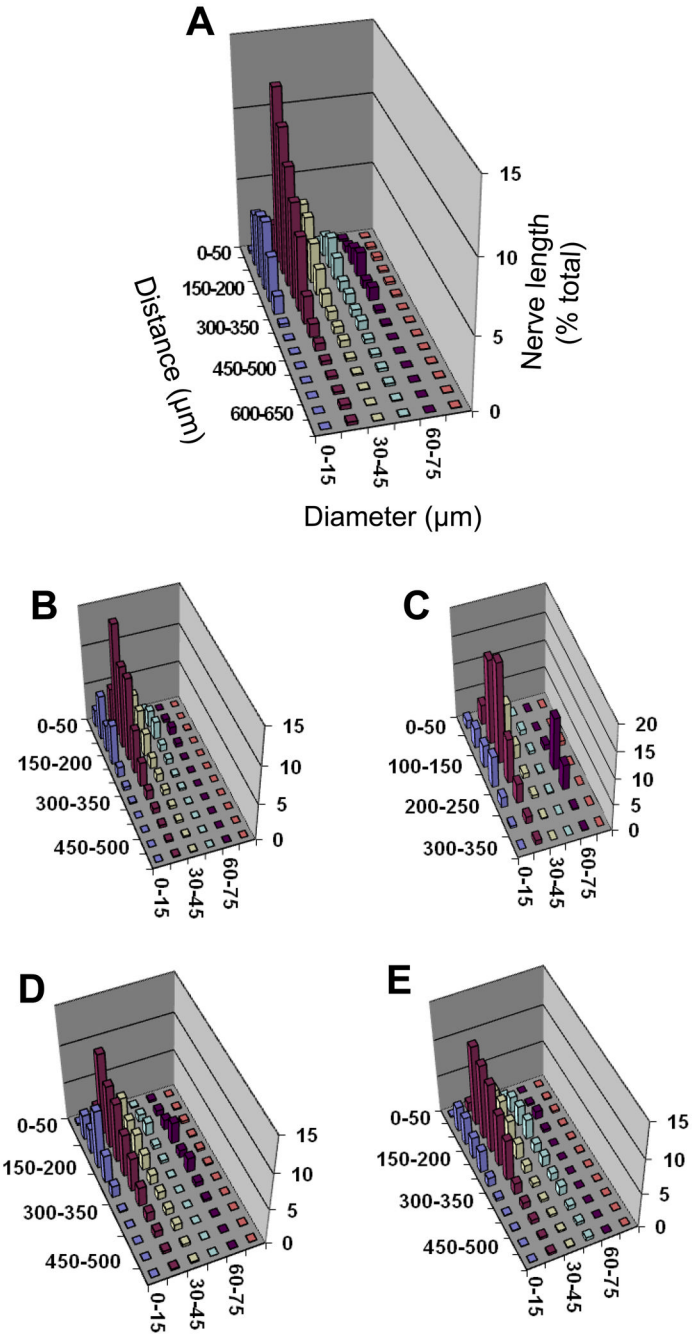


**Figure 2. Proximity analyses between motor nerves and arterioles for diaphragm muscle of C57BL/6 mice**

Separation distance between a nerve fiber and its nearest arteriole (Z axis) expressed as percentage of total nerve length (Y axis) according to arteriolar diameter (X-axis). Relationships are shown for: **A.** Entire diaphragm muscle; **B.** Costal muscle region; **C.** Crural muscle region; **D.** Right hemidiaphragm; **E.** Left hemidiaphragm. Axes labels for **A** apply to other panels; note difference in Y-axis and Z-axis scales. The greatest % of nerve length is associated with arterioles ≤ 45 μm diameter within a distance ≤ 250 μm. The peak for larger arterioles (diameter, 60–75 μm) in the crural region corresponds to entry of

inferior phrenic artery into the diaphragm muscle. The height of each bar corresponds to the mean of n=4 preparations. Error bars omitted for clarity; variability shown in Fig. 4.

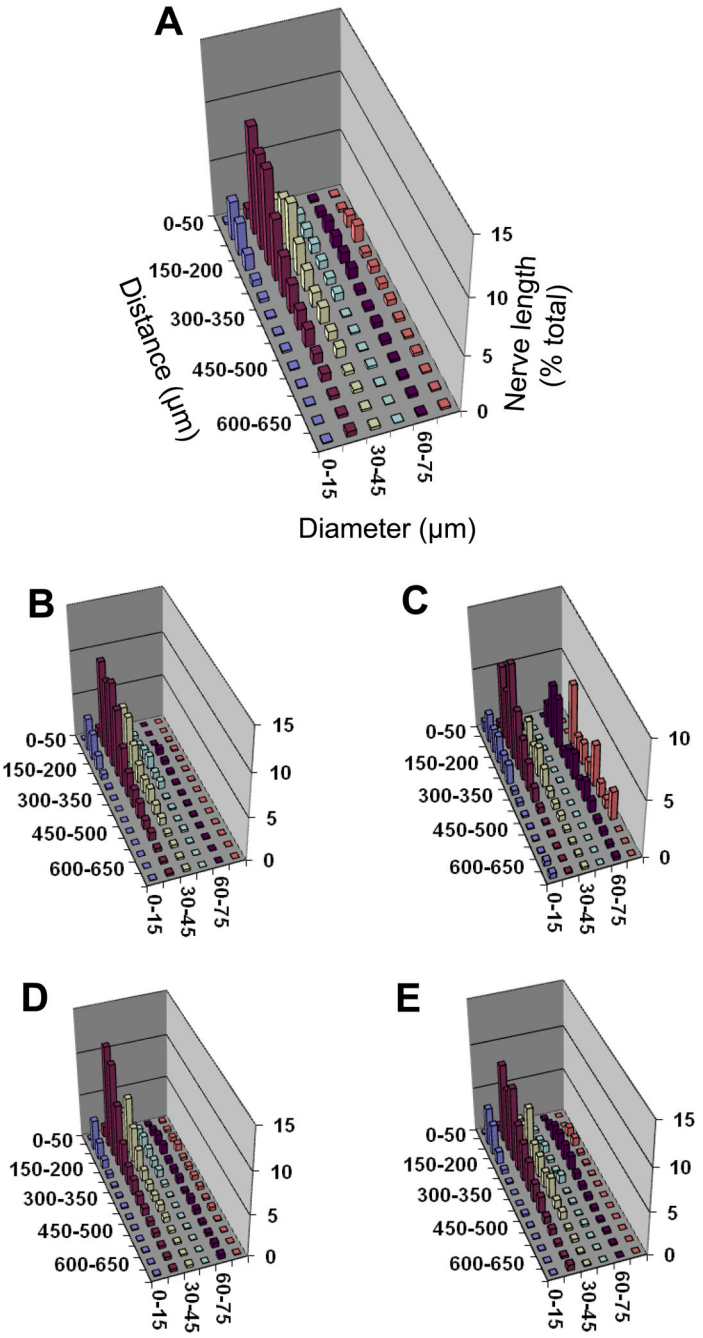


**Figure 3. Proximity analyses between motor nerves and arterioles for diaphragm muscle of CD-1 mice**

Separation distance between a nerve fiber and its nearest arteriole (Z axis) expressed as percentage of total nerve length (Y axis) with respect to vessel diameter (X-axis). Relationships are shown for: **A.** Entire diaphragm muscle; **B.** Costal muscle region; **C.** Crural muscle region; **D.** Right hemidiaphragm; **E.** Left hemidiaphragm. Axes labels for **A** apply to other panels; note difference in Y-axis scales. The greatest % of nerve length is associated with vessels ≤ 45 μm diameter within a distance ≤ 250 μm. The peak for larger vessels (diameter ≥ 60–75 μm) in the crural region corresponds to entry of inferior phrenic

artery into the muscle. The height of each bar corresponds to the mean of n=4 preparations. Error bars omitted for clarity; variability shown in Fig. 4.

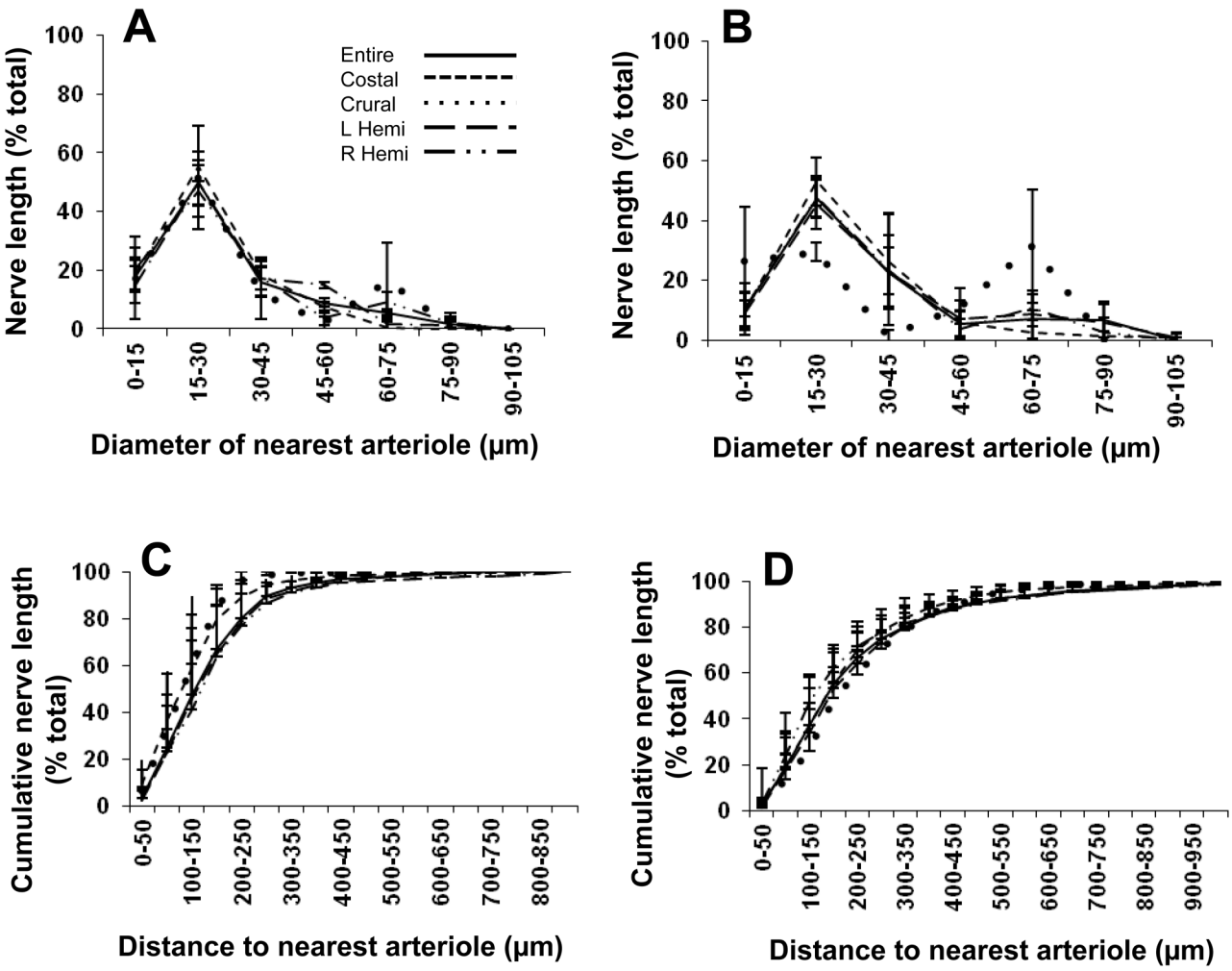


**Figure 4. Neurovascular association in mouse diaphragm muscle**

For each panel, summary data (means ± S.D.; n=4 per group) are presented for the entire muscle and for respective muscle regions. **A.** The percentage of total phrenic nerve length associated with arterioles of respective diameters in C57BL/6 mice. The majority of nerve branches associate with arterioles 15–30 μm in diameter. **B.** As in **A** for CD-1 mice. For the entire muscle, 84 ± 2% (C57BL/6) and 80 ± 10% (CD-1) of total nerve length associated with arterioles ≤ 45 μm. **C.** Ogive for percentage of total nerve length in relation to distance to the nearest arteriole in C57BL/6 mice. **D.** As in **C** for CD-1 mice. For the entire muscle, 80 ± 14% (C57BL/6) and 67 ± 10% (CD-1) of total nerve length is located within 250 μm from the nearest arteriole. Legend in **A** applies to all panels.

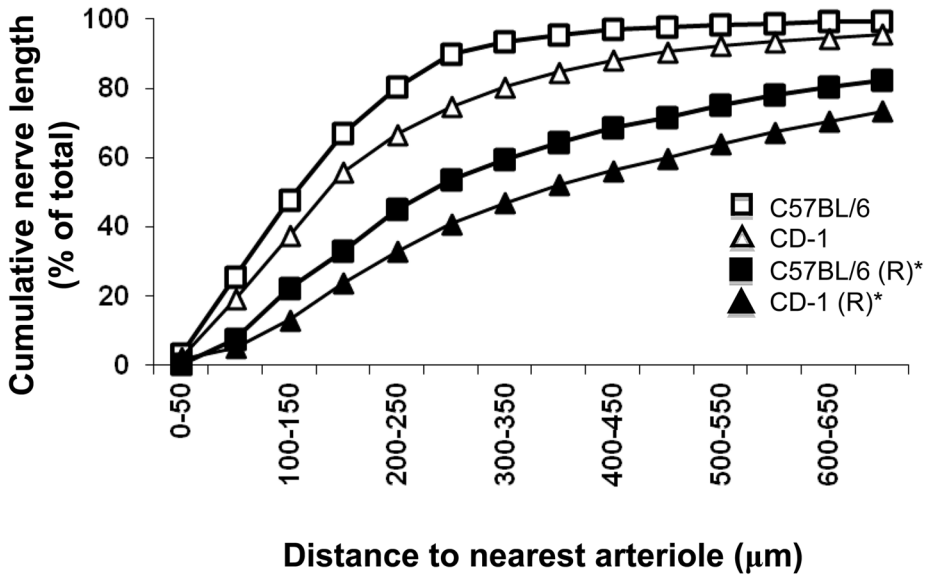


**Figure 5. Distances to nearest arteriole within which 50% of total phrenic nerve length occurs in mouse diaphragm muscles**

The $D_{50}$ obtained in control preparations (C57BL/6, 155 ± 30 μm; CD-1, 199 ± 22 μm) nearly doubled after repositioning (R) nerve networks relative to respective control vascular networks within muscle borders (C57BL/6, 286 ± 77 μm; CD-1, 386 ± 64 μm). *$P < 0.05$ for repositioned vs. control in both C57BL/6 and CD-1 mice.

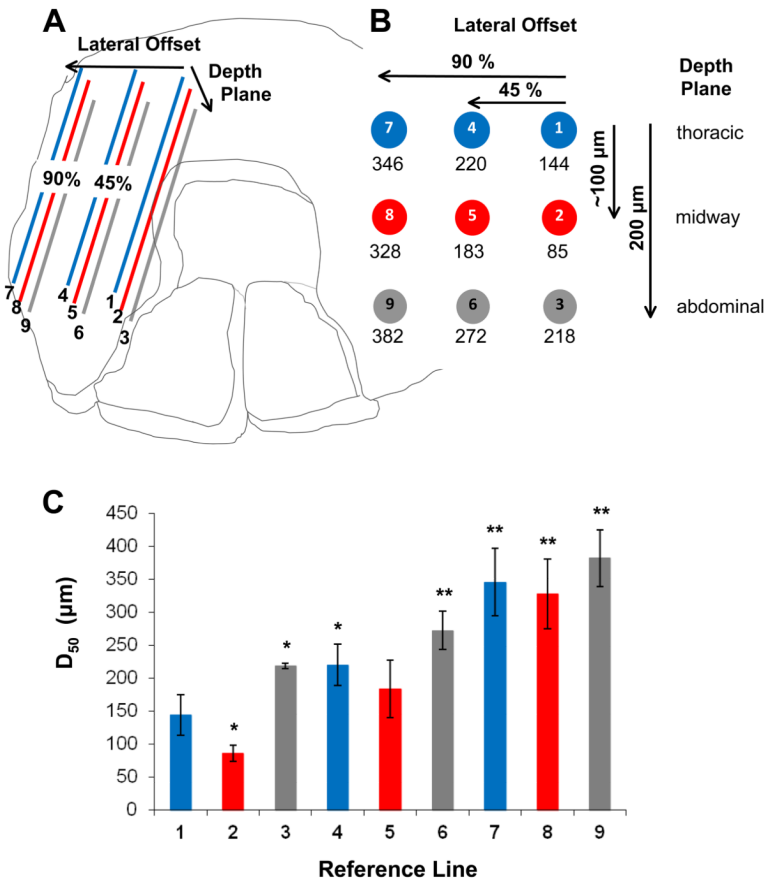


**Figure 6. Independent reference lines for nerve position**

**A**. Nine reference lines were positioned through the thickness (~200 μm) and across the width (~8 mm) of the left costal region of each diaphragm muscle studied in C57BL/6 mice; each line represented 75% of actual nerve length for that muscle region. Through the muscle thickness, reference lines represent three planes: adjacent to thoracic surface (corresponding to the nerve plane), midway through the muscle thickness (corresponding to the arteriolar plane) and adjacent to abdominal muscle surface (deepest plane relative to nerve plane). Within each reference plane, lines were positioned at 45% and 90% of the distance (Lateral Offset) to the costal muscle boundary. **B**. End view illustrates position of reference lines within muscle boundaries with mean respective $D_{50}$ values determined according to Figure 5. For actual nerves, the $D_{50}$ value was 155 ± 30 μm. **C**. Histogram showing $D_{50}$ values calculated for each reference line. *P<0.05 vs. actual nerves; ** P<0.01 vs. actual nerves.